Electronic Supplementary Material (ESI) for Journal of Materials Chemistry C.

Supporting Information

White Light Emission and Temperature Dependent Chromaticity Shifts by Modification of Luminescent ZrO(FMN) Nanoparticles with Rare Earth Halides

T. Wehner,[a] J. Heck,[b] C. Feldmann[b] and K. Müller-Buschbaum*[,a]

a. Institut für Anorganische Chemie, Universität Würzburg, Am Hubland, 97074 Würzburg, Germany. E-Mail: k.mueller-buschbaum@uni-wuerzburg.de

b. Institut für Anorganische Chemie, Karlsruher Institut für Technologie (KIT), Engesserstraße 15, 76131 Karlsruhe, Germany. E-Mail: claus.feldmann@kit.edu

Photoluminescence Spectroscopy

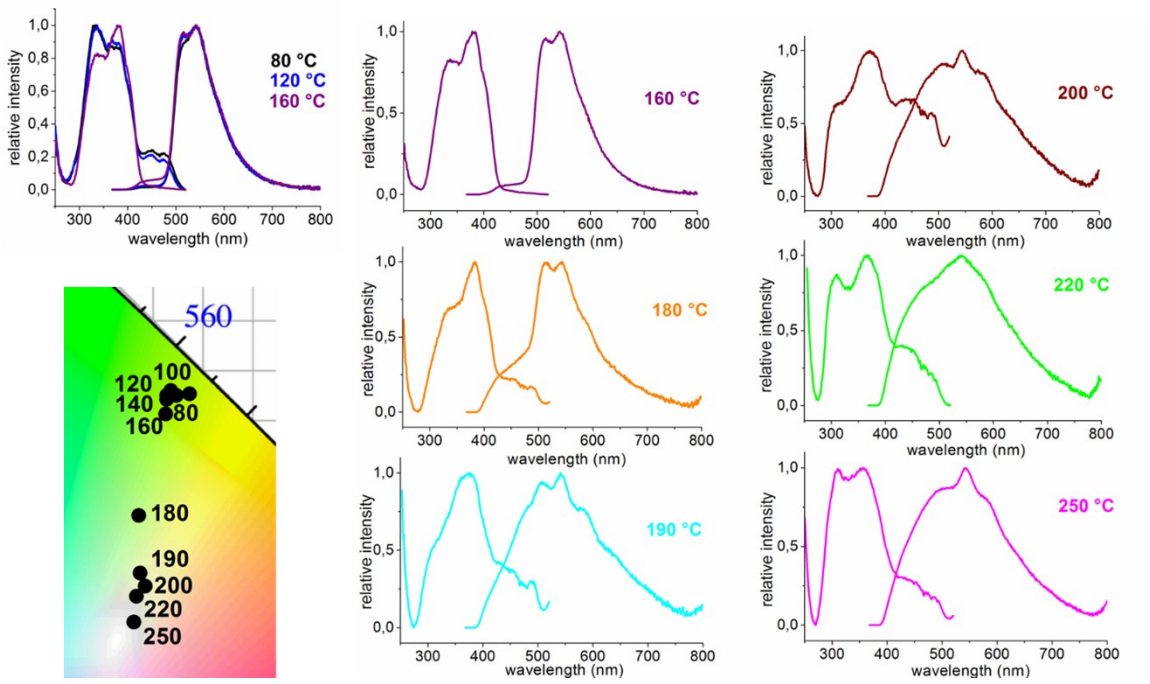

Figure S1. Excitation and emission spectra of ZrO(FMN)/$LaCl_3$/py at different reaction temperatures and the resulting shift of the chromaticity of the modified particles.

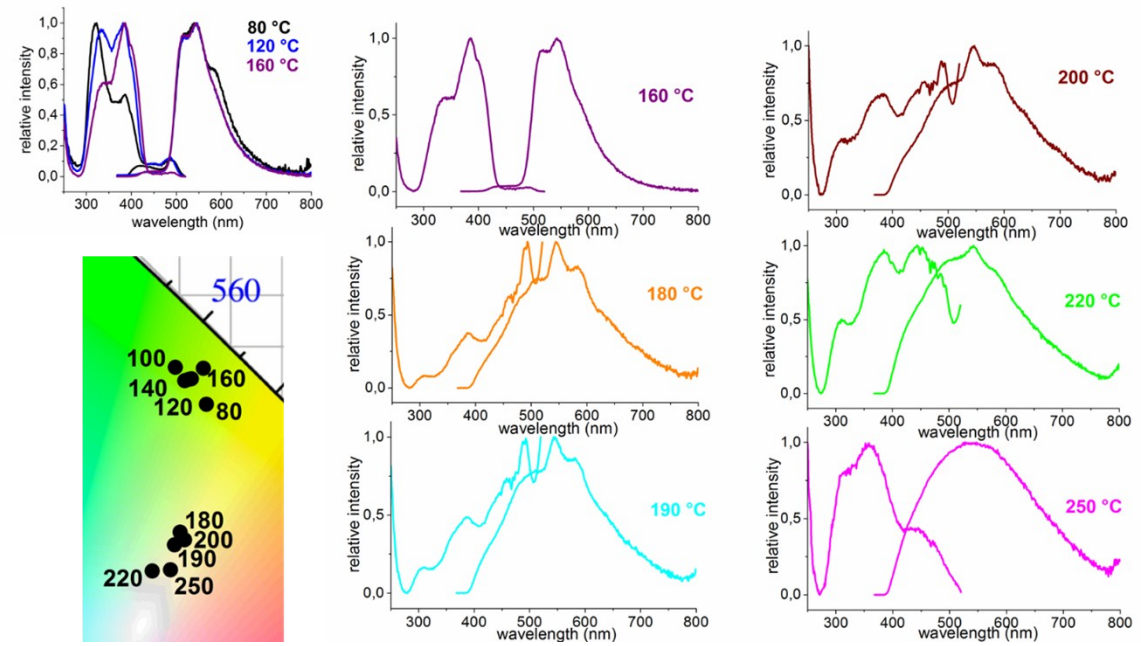

Figure S2. Excitation and emission spectra of ZrO(FMN)/$HoCl_3$/py at different reaction temperatures and the resulting shift of the chromaticity of the modified particles.

Photoluminescent Lifetime

Table S1. Photoluminescent lifetimes of different suspensions excited at 375 nm.

Sample	λ_{em}/nm	B_1/%	τ_1	B_2/%	τ_2	χ^2
ZrO(FMN)/py	550	30.09	1.349 ns (0.010)	69.91	5.585 ns (0.015)	1.48
ZrO(FMN)/YCl_3/py (T = 180 °C)	550	100	5.163 ns (0.004)	/	/	1.19
ZrO(FMN)/YCl_3/py (T = 230 °C)	550	60.02	4.010 ns (0.023)	39.98	8.897 (0.065)	1.14

λ_{em}: the emission wavelength that the decay was monitored.

B: the percentage contributions of different decay processes.

χ^2: the wellness of the exponential fits to the raw data.

Values in parentheses indicate the standard deviations of the lifetime.

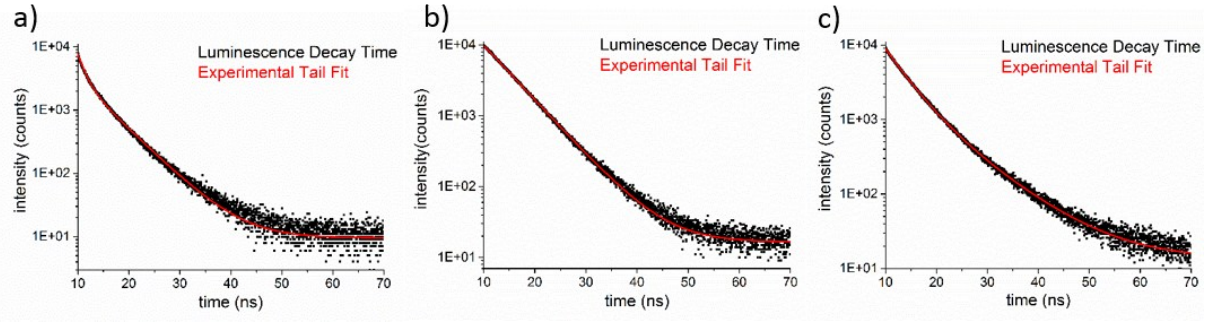

Figure S3. Photoluminescent lifetime decay curves and experimental tail fit of different suspensions excited at 375 nm (λ_{em} = 550 nm) a) ZrO(FMN)/py; b) ZrOFMN/YCl_3/py (T = 180 °C); c) ZrOFMN/YCl_3/py (T = 230 °C)

Low Temperature Photoluminescence Spectroscopy

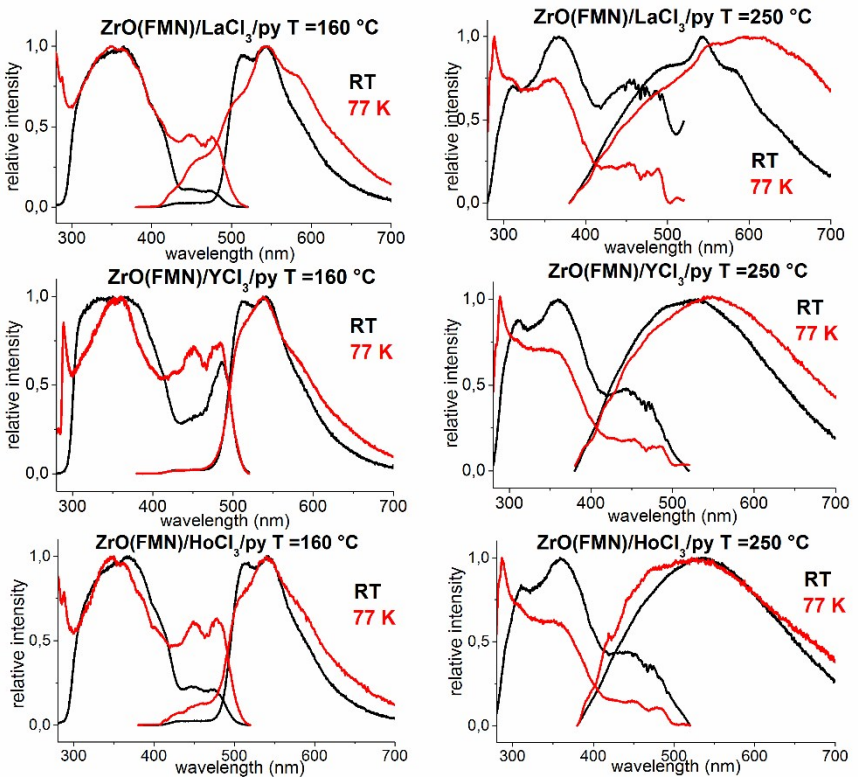

Figure S4. Excitation and emission spectra of ZrO(FMN)/$LnCl_3$/py (for reaction temperatures of 160 °C and 250 °C), recorded at RT and -196 C, Ln = La, Y, Ho.

XRF Analysis

Table S2. Exemplary EDXS studies of the reaction products of ZrO(FMN) with $LnCl_3$, Ln = La, Ho. The samples contain additional amounts of Si caused by the sample holder (not listed below).

ZrO(FMN) + HoCl3		**ZrO(FMN) + LaCl3 + NEt3**	
Element	At%	Element	At%
C K	56.25	C K	41.71
O K	13.37	O K	26.07
P K	0.37	N K	7.13
Ho M	1.46	La M	8.84
Zr L	0.22	Zr L	1.08
Cl K	2.65	Cl K	3.55

Table S3. XRF study of the modification products of ZrO(FMN) with $LaCl_3$ showing a significantly higher Zr content as compared to EDXS. The samples also contain amounts of Si that is caused by the sample holder.

Element	At%
P K	8.55
Cl K	48.61
La L	22.46
Zr K	16.42

Powder X-Ray Diffraction

PXRD analysis was carried out on both the precipitates and dried dispersions of the ZrO(FMN)/$LnCl_3$ systems. In addition to an amorphous background, which is caused by the nanoparticular composites, the reaction products show reflections, which indicate the formation of different side phases due to nanoparticle decomposition. An assignment of the different side phases to different reaction products can be found in Table 1. Some of the identified phases can only be detected in very low amounts and thus show very weak reflections.

Table S4. Assignment of precipitates and dispersions of different ZrO(FMN)/$LnCl_3$ systems(Ln = La, Y, Ho) to the identified side phases.

	180 °C	**230 °C**
Ln=La, precipitate	$La(PO_4)$, LaOCl, $Zr(H_2PO_2)_3$	$La(PO_4)$
Ln=Y, precipitate	unknown phase(s)	$Y(PO_4)$, $Zr(HPO_4)_2$, YHP_2O_7, $Y(PO_3)_3$, $(ZrO_2)_{0.98}(Y_2O_3)_{0.02}$
Ln=Ho, precipitate	unknown phase(s)	unknown phase(s)
Ln=La, dispersion	completely amorphous	completely amorphous
Ln=Y, dispersion	unknown phase(s)	$Zr(Y(PO_4)$, $Zr(HPO_4)_2$, YHP_2O_7, $Y(PO_3)_3$, $(ZrO_2)_{0.98}(Y_2O_3)_{0.02}$
Ln=Ho, dispersion	unknown phase(s)	unknown phase(s)

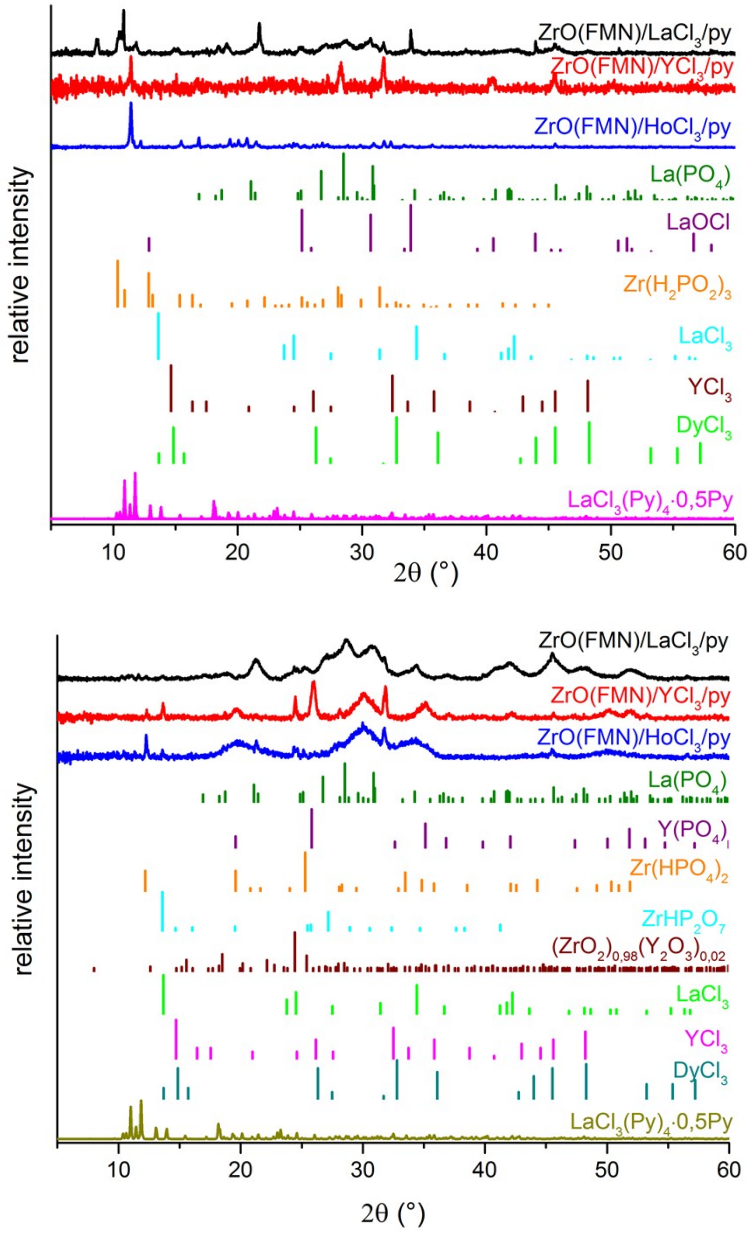

Figure S5. Powder diffraction patterns of the precipitates of the systems ZrO(FMN)/$LnCl_3$/py at 180 °C (top) and 230 °C (bottom) in comparison with different Ln and Zr chlorides, oxides and phosphates. The diffractograms were corrected for the amorphous background.

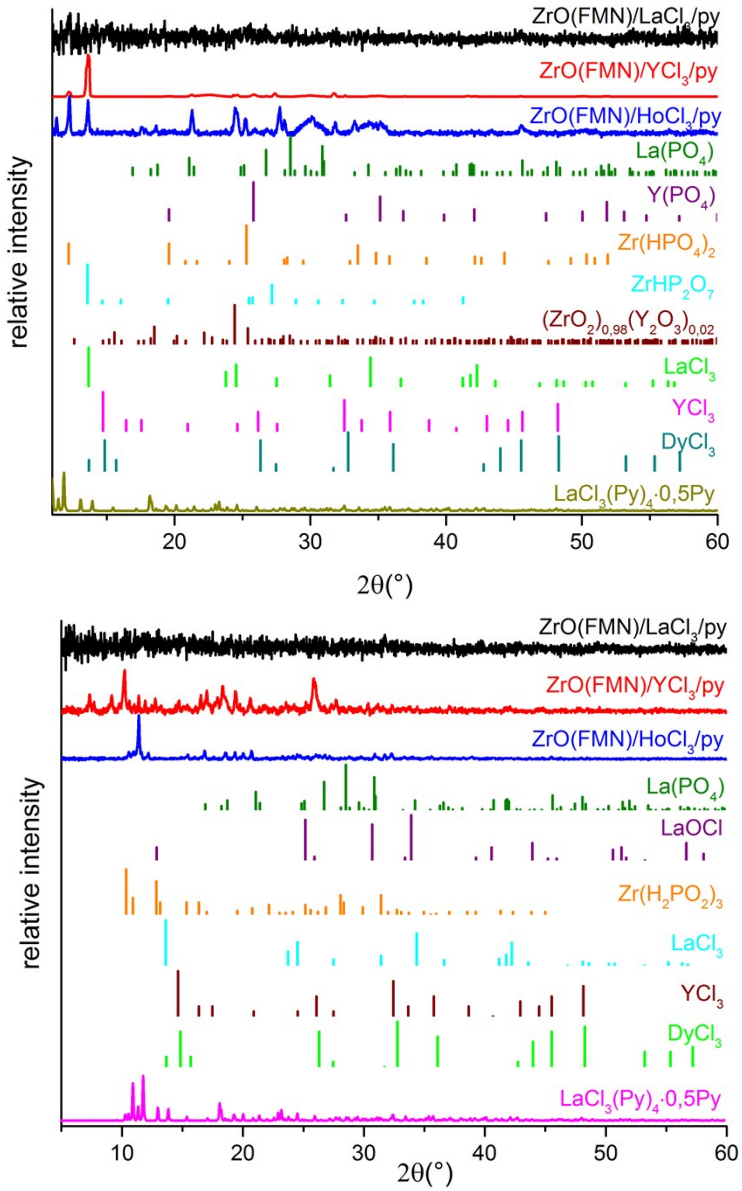

Figure S6. Powder diffraction patterns of dispersions of ZrO(FMN)/$LnCl_3$/py heated to 180 °C (top) and 230 °C (bottom) and after solvent removal in comparison with different Ln and Zr chlorides, oxides and phosphates.

IR Spectroscopy

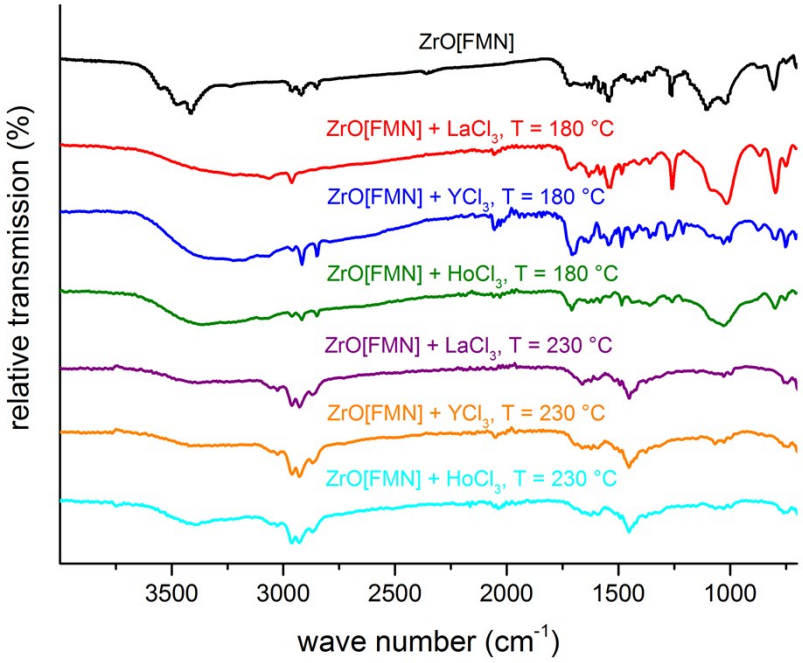

Figure S7. Infra-red spectra of dispersions of $LnCl_3$/ZrO(FMN)/py after solvent removal in comparison to unmodified ZrO(FMN) dried from suspensions in py.

NMR Spectroscopy

NMR signals of ZrO(FMN), dried from pyridine:

^{1}H-NMR (300.18 MHz, pyridine-d6), δ, ppm: 8.76-8.69 (s, 2H), 7.58-7.51 (m, 1H), 7.20-7.16 (s, 2H).

^{13}C{^{1}H}-NMR (75.48 MHz, pyridine-d6, δ, ppm: 149.65 (s, 2H), 134.93 (s, 1H), 123.25 (s, 2H).

NMR signals of $LaCl_3$@ZrO(FMN), dried from pyridine:

^{1}H-NMR (300.18 MHz, pyridine-d6), δ, ppm: 8.48 (s, 2H), 7.35-7.29 (m, 1H), 6.98-6.93 (s, 2H).

^{13}C{^{1}H}-NMR (75.48 MHz, pyridine-d6, δ, ppm: 150.00 (s, 2H), 135.25 (s, 1H), 123.58 (s, 2H).